

# Quantifying the Jet Energy Loss in Pb+Pb collisions at LHC

Vineet Kumar<sup>1,2\*</sup> and Prashant Shukla<sup>1,2\*</sup>

<sup>1\*</sup>Nuclear Physics Division, Bhabha Atomic Research Center, Mumbai, 400085, Maharashtra, India.

<sup>2</sup>Homi Bhabha National Institute, Training School Complex, Anushaktinagar, Mumbai, 400094, Maharashtra, India.

\*Corresponding author(s). E-mail(s): [pshukla@barc.gov.in](mailto:pshukla@barc.gov.in);

## Abstract

In this work, we give a method to study the energy loss of jets in the medium using a variety of jet energy loss observables such as nuclear modification factor and transverse momentum asymmetry in dijets and  $\gamma$ -jets in heavy ion collisions. The energy loss of jets in the medium depends mainly on the size and the properties of medium viz. temperature and is a function of energy of the jets as predicted by various models. A Monte Carlo (MC) method is employed to generate the transverse momentum and path-lengths of the initial jets that undergo energy loss. Using different scenarios of energy loss, the transverse momentum and system size dependence of nuclear modification factors and different measures of dijet momentum imbalance at energies  $\sqrt{s_{NN}} = 2.76$  TeV and 5.02 TeV and  $\gamma$ -jet asymmetry at  $\sqrt{s_{NN}} = 2.76$  TeV in Pb+Pb collisions are simulated. The results are compared with the measurements by ATLAS and CMS experiments as a function of transverse momentum and centrality. The study demonstrates how the system size and energy dependence of jet energy loss can be quantified using various experimental observables.

**Keywords:** quark-gluon plasma, LHC, Jet

# 1 Introduction

The PbPb collisions at Large Hadron Collider (LHC) are performed to produce and study the properties of bulk strongly interacting matter at high temperatures where the quarks and gluons provide the basic degrees of freedom [1]. The matter in this phase is called quark gluon plasma (QGP) which is short-lived but leaves its imprints on many observables which are captured by gigantic multi particle detectors. The experimental probes are categorised in terms of soft probes which determine the global properties of the system and hard probes which give tomography of the system; jets are in the later category. When two hadrons collide at high energies, the hard scattering of partons produces two virtual back-to-back partons. These partons subsequently evolve as parton showers, hadronize and are observed as two back-to-back hadronic jets. In heavy ion collisions, the quarks and gluons produced in the hard scattering interact strongly with the hot QCD medium due to their color charges, and lose energy, either through the collisions with medium partons or through gluon bremsstrahlung [2, 3]. The jet properties are thus modified in heavy ion collisions, a phenomenon which is termed as jet-quenching [4]. Since the hard partonic scattering occurs early in the collisions, the produced jets probe the medium properties such as stopping power and transport coefficients. The jet-quenching can be quantified in many ways. The most conventional way is the nuclear modification factor  $R_{AA}$  which is defined as the ratio of number of jets in heavy ion collisions to the suitably scaled number of jets in pp collisions. The nuclear modification factor for light hadrons at high  $p_T$  is also a measure of jet-quenching at RHIC [5] and at LHC [6–8]. The  $R_{AA}$  values for hadrons at RHIC and the LHC are very similar although one would expect the energy loss to increase with increased collision energy. QCD-motivated models are generally able to describe inclusive single particle  $R_{AA}$  qualitatively.

The fully reconstructed jets have allowed to measure the momentum imbalance between the leading and sub-leading jet in each event which are quantified using dijet asymmetry variables. Due to kinematic and detector effects, the observed energy of dijets is not perfectly balanced, even in pp collisions. Thus to obtain a quantitative measure of the dijet imbalance, systematic comparison of results from heavy ion collisions with pp collisions are done. The dijet measurements from the ATLAS [9] and CMS [10, 11] show that, the distributions of dijet asymmetry for peripheral PbPb collisions are similar to those from pp collisions but are broader for central PbPb collisions. Recently, ATLAS measured jet imbalance after background subtraction and applied unfolding procedure to account for experimental effects [12, 13] with similar conclusions. A recent measurement from ATLAS gives substructure-dependent jet suppression in Pb+Pb collisions at 5.02 TeV [14]. There have also been results from RHIC; The measurements from STAR experiment [15] using a high momentum component selection ( $p_T \geq 2$  GeV/c) observed the similar energy imbalance seen by ATLAS and CMS. With the large statistics data collected during the PbPb runs of the LHC at 5.02 TeV, the measurements of  $\gamma$ -jet and  $Z^0$ -jet pairs have become accessible. Both the photon and  $Z^0$  do not participate in strong interactions and hence escape the medium unattenuated and thus the energy of the paired jet can be determined precisely. The CMS measurement [16] of isolated photons with  $p_T \geq 60$  GeV/c and associated jets with  $p_T \geq 30$  GeV/c in PbPb collisions at  $\sqrt{s_{NN}} = 2.76$  TeV demonstrates that

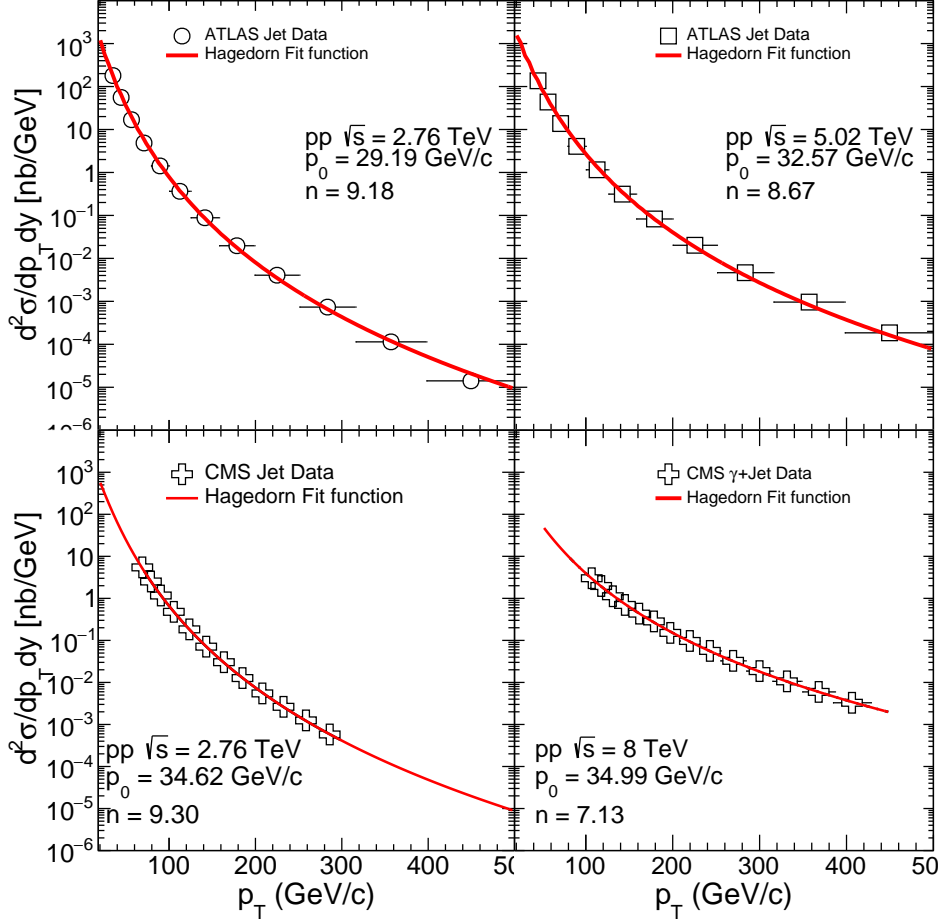


**Fig. 1** (Color online) Jet yields as a function of jet  $p_T$  in pp collisions measured by ATLAS [18, 19] and CMS experiments [17, 20]. The lines correspond to Hagedorn fit, the parameters of which are given in the figure.

jet loses energy increasingly with increasing centrality. Recent measurements of Z boson-tagged jets in PbPb collisions at  $\sqrt{s_{NN}} = 5.02$  TeV [17], although with limited statistics, show that the transverse momentum of the jet shifts to lower values.

There are many approaches to describe the jet-medium interactions. In Gyulassy-Levai-Vitev (GLV) formalism [21, 22], a systematic expansion in opacity is used to extract the radiative energy loss of partons inside QGP which has logarithmic dependence on jet energy. In the Baier-Dokshitzer-Peigne-Schiff (BDPS) approach, a fast parton radiates gluon by multiple coherent scatterings in the thick medium [2]. The finite medium effect was discussed in BDMPs work [23, 24]. Phenomenological models of parton energy loss [25] in QGP tend to define simple dependence of the radiative energy loss of the parton on the energy of the parton inside the medium. The energy

loss can be characterized in terms of coherence length  $l_{\text{coh}}$ , which is associated with the formation time of gluon radiation by a group of scattering centres, the mean free path ( $\lambda$ ) of the parton and the medium size  $L$  [26, 27]. If  $l_{\text{coh}} < \lambda$ , the energy loss per unit length is proportional to the energy of the parton which is known as Bethe-Heitler regime. The regime  $l_{\text{coh}} > \lambda$  corresponds to Landau-Pomeranchuk-Migdal (LPM) regime where the energy loss per unit length is proportional to the square-root of the incoming parton energy. If  $L \gg l_{\text{coh}}$ , the energy loss per unit length is proportional to the square root of the energy of the parton (BDPS result). For  $L \ll l_{\text{coh}}$ , the energy loss per unit length is independent of energy but proportional to the parton path length. These simple dependencies have been used to explain the charged particle spectra at RHIC and LHC in heavy ion collisions [28, 29].

Recently the fragmentation of partons propagating in a dense quark gluon plasma is studied using leading double logarithmic approximation in perturbative QCD [30]. The effects of the medium on multiple vacuum like emissions is found to modify the in medium parton showers in comparison to the vacuum showers [30]. These modified parton showers are then used to study the jet nuclear modification factor  $R_{AA}$  and the distributions of jet splitting function  $Z_g$  at LHC energies using Monte Carlo methods [31]. It is found that the energy loss by the jet is increasing with the jet transverse momentum, due to a rise in the number of partonic sources via vacuum like emissions [31]. Another consequence of the jet substructure modification inside QGP will demonstrate itself through the cone size dependence of jet energy loss. An analytical description has been obtained for the cone size dependent jet spectrum in heavy ion collisions at the LHC energies implemented in a event by event setup including hydrodynamic expansion of the quark gluon plasma and accounting for multiple scattering effects [32]. The calculation yields a good description of the centrality and  $p_T$  dependence of jet suppression for  $R = 0.4$  together with a mild cone size dependence, which is in agreement with recent experimental results [32].

The measured  $R_{AA}$  of jets is used to obtain energy loss of jets in many phenomenological studies [33–35]. Such studies assume that the energy loss is given by a power law in terms of  $p_T$  and the value of power index is obtained by fitting the  $R_{AA}$  as a function of  $p_T$  and centrality. In Ref.[36], the power law function is applied to describe the transverse momentum distributions of charged particles and jets in heavy ion collisions which includes the transverse flow in low  $p_T$  region and the in-medium energy loss (also in terms of power law) in high  $p_T$  region. The jet-quenching is quantified using jet nuclear modification factors in various kinematic regions in terms of parameters of a power law function assumed for energy loss [37]. Although there are simulation packages like JETSCAPE [38] which deal with the system more elaborately but simple models provide easy alternatives to characterize the essential features of energy loss using different variables in different collisions systems.

In this work, we have proposed a method which calculates experimental energy loss probes namely dijet asymmetry as well as  $R_{AA}$  taking different energy loss prescriptions as inputs. The aim is to obtain the energy loss dependence on variables like transverse momentum and centrality. We obtain the parameters of these energy loss formulas from experiments hence quantifying the energy loss. Once the parameters are

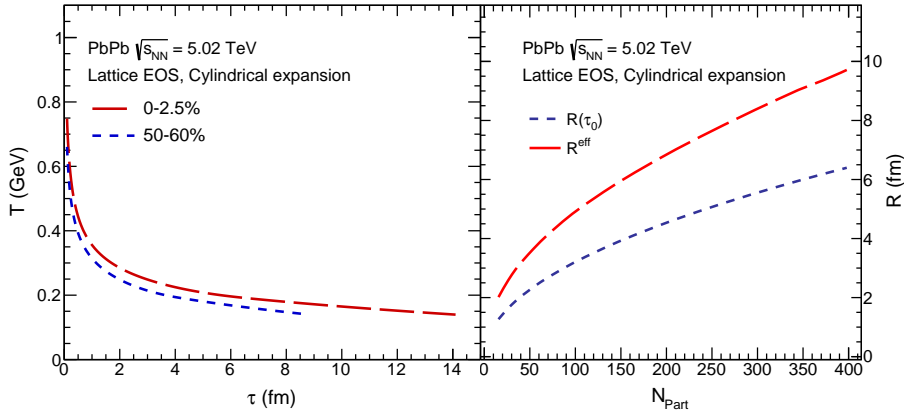


**Fig. 2** (Color online) (left) Temperature in the system as a function of proper time  $\tau$  in cases of the central (0-2.5%) and peripheral (50-60%) collisions for cylindrical expansions using the lattice equation of state. (right) Transverse size of the system as a function of  $N_{\text{Part}}$  of the collisions. The dashed blue line shows the transverse size,  $R(\tau_0)$ , at the initial time  $\tau_0$  while long dashed red line shows the effective transverse size,  $R^{\text{eff}}$ , obtained by integrating the  $R(\tau)$  over the time evolution of the system.

obtained by fitting over large datasets it has excellent predictive power in other kinematics regions. The aim of comparing the measurements at different collision energy and by different experimental group is to bring out the underlying difference due to physics or due to different method of analysis affecting the energy loss probes. We assume that the energy loss of jets in the hot medium is a function of jet energy in the form of power law where the power index is extracted using the  $R_{AA}$  and dijet asymmetry data from the LHC. In addition, we use (GLV) form of energy loss which is logarithmic in energy [21, 22]. Determining the pathlength of the jets in the medium is equally important to know the energy loss suffered by jets. Guided by these considerations, Monte Carlo method is employed to generate the jet  $p_T$  which travel certain pathlength in the medium and lose energy. Different forms of energy loss are used to obtain dijet and  $\gamma$ -jet asymmetry and nuclear modification factor in the PbPb collisions at two LHC energies.

## 2 Jet energy loss

To describe the transverse momentum distribution of jets in pp collisions, Hagedorn function is used which is given by [37, 39]

$$\frac{d^2\sigma}{dp_T dy} = 2\pi p_T \frac{dn}{dy} \left(1 + \frac{p_T}{p_0}\right)^{-n}. \quad (1)$$

Figure 1 shows the jet yields as a function of jet  $p_T$  in pp collisions measured by ATLAS [18, 19] and CMS experiments [17, 20]. The lines correspond to Hagedorn fit. The parameters  $n$  and  $p_0$  obtained by fitting the  $p_T$  distribution of jets are given on the

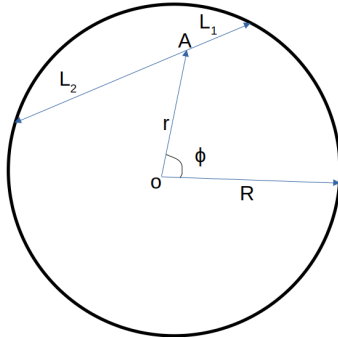


**Fig. 3** (Color online) Snapshot of transverse cross section of the expanding QGP medium, two back-to-back jets produced at radial distance  $r$  traversing different path-lengths in the medium.

Fig. 1. These measured  $p_T$  distributions parameterized with the Hagedorn fit (Eq. 1) along with the measured asymmetry in pp data are used to calculate the initial jets transverse momenta ( $p_T$ ).

The specific energy loss,  $dE/dx$  is modeled as a power law in  $p_T$  of jet [37]

$$\frac{dE}{dx} = M \left( \frac{p_T}{p_{T0}} - C \right)^\alpha. \quad (2)$$

The index  $\alpha$  decides the energy dependence of jet energy loss and the parameter  $M$  is dependent on medium properties such as the temperature of QGP e.g.  $\frac{M}{\sqrt{p_{T0}}} \sim C_R \alpha_S \sqrt{\mu^2/\lambda}$  in BDPS formalism [2]. Here,  $p_{T0}$  is a scale set to 1 GeV/ $c$  and value of  $C = 0$ .

We also used GLV formalism [21, 22] of parton energy loss inside QGP. In this formalism, the energy loss is given by

$$\frac{\Delta E}{L} = \frac{C_R \alpha_S}{N(E)} \frac{L \mu^2}{\lambda} \log \frac{E}{\mu}. \quad (3)$$

Here,  $C_R$  is the color factor for quarks and gluons. The QCD values of color factors are  $4/3$  ( $C_{Rq}$ ) and  $3$  ( $C_{Rg}$ ) for quarks and gluons respectively. We use a weighted average for  $C_R$  such as

$$C_R = f_q C_{Rq} + (1 - f_q) C_{Rg} \quad (4)$$

where  $f_q$  is  $p_T$  dependent quark fraction calculated using PYTHIA [40] in ref. [41]. The  $\alpha_S$  ( $= 0.3$ ) represents the QCD coupling constant,  $\lambda$  is mean free path of parton inside the QGP,  $\mu^2$  ( $= 4\pi\alpha_S T^2(1 + N_f/6)$ ) is thermal gluon mass. The factor  $N(E)$  encoded the effect of finite kinematics on radiative energy loss which causes it to deviate considerably from the asymptotic value of 4 [21]. The value of  $N(E)$  has slow dependence at parton energy as  $N(E) = 24.4, 10.1, 7.3, 4.0$  for  $E = 5, 50, 500, 1000$  GeV, respectively. We use linear interpolation to determine the values of  $N(E)$  at intermediate energies.

The mean free path  $\lambda$  is given by

$$\lambda^{-1} = \rho_g \sigma_{Qg} + \rho_q \sigma_{Qq}, \quad (5)$$

where

$$\rho_g = 16 T^3 \frac{1.202}{\pi^2}, \quad \rho_q = 9 N_f T^3 \frac{1.202}{\pi^2}, \quad (6)$$

$$\sigma_{Qq} = \frac{9\pi\alpha_s^2}{2\mu^2} \text{ and } \sigma_{Qg} = \frac{4}{9}\sigma_{Qq}. \quad (7)$$

The  $\rho_g$  and  $\rho_q$  are the quark and gluon densities inside the QCD medium,  $\sigma_{Qg}$  and  $\sigma_{Qq}$  represents cross section of quark quark and quark gluon interaction. The values of  $N_f (= 3)$  and  $N_C (= 3)$  are used in the calculations [42]. At  $T_{\text{eff}} = 0.212(0.220)$  GeV, the values of the parameters are  $\mu = 0.504(0.523)$  GeV and  $\lambda = 1.21(1.17)$  fm.

The evolution of the system for each centrality class is governed by an isentropic cylindrical expansion ( $s(T)V(\tau) = s(T_0)V(\tau_0)$ ) with prescription given in Ref. [43]. The equation of state (EOS) obtained by Lattice QCD and hadronic resonances is used [44]. The transverse size  $R$  for a given centrality with number of participant  $N_{\text{Part}}$  is obtained as  $R(N_{\text{Part}}, \tau_0) = R_A \sqrt{N_{\text{Part}}/2A}$ , where  $R_A$  is radius of the nucleus. The initial entropy density,  $s(\tau_0)|_{0-2.5\%}$ , for 0-2.5% centrality is

$$s(\tau_0)|_{0-2.5\%} = \frac{a_m}{V(\tau_0)|_{0-2.5\%}} \left( \frac{dN}{d\eta} \right)_{0-2.5\%}. \quad (8)$$

Here  $a_m (= 5)$  is a constant which relates the total entropy to the total multiplicity  $dN/d\eta$  obtained from hydrodynamic calculations [45]. The volume element  $V(\tau) = \tau \pi (R(\tau))^2$  is given by

$$V(\tau) = \tau \pi \left( R(\tau_0) + \frac{1}{2} a_T \tau^2 \right)^2, \quad (9)$$

where  $a_T = 0.1 c^2 \text{ fm}^{-1}$  is the transverse acceleration [43]. We estimate the initial temperature,  $T_0$ , in the 0-2.5% most central collisions from the total multiplicity in the rapidity region of interest, assuming that the initial time is  $\tau_0 = 0.1 \text{ fm}/c$  over all rapidities. The total multiplicity in a given rapidity region is 1.5 times the charged particle multiplicity in PbPb collisions. With the lattice EOS, at midrapidity, with  $(dN_{\text{ch}}/d\eta)_{0-2.5\%} = 1943$  [46], we find  $T_0 = 0.606$  GeV at  $\sqrt{s_{\text{NN}}} = 5.02$  TeV. At  $\sqrt{s_{\text{NN}}} = 2.76$  TeV  $(dN_{\text{ch}}/d\eta)_{0-2.5\%}$  and  $T_0$  are 1620 and 0.571 GeV respectively.

Figure 2 (left) shows temperature in the system as a function of proper time  $\tau$  in case of the central (0-2.5%) and peripheral (50-60%) collisions for cylindrical expansions using the lattice equation of state. The temperature is averaged over the time evolution of the system for each centrality class to extract the effective temperature,  $T_{\text{eff}}$ . The  $T_{\text{eff}}$  is similar for all the centrality classes because longer life time of QGP compensates for higher initial temperature  $T_0$  in central collisions as shown in Figure 2. The calculated values of  $T_{\text{eff}}$  are 0.220 GeV and 0.212 GeV at  $\sqrt{s_{\text{NN}}} = 5.02$  and 2.76

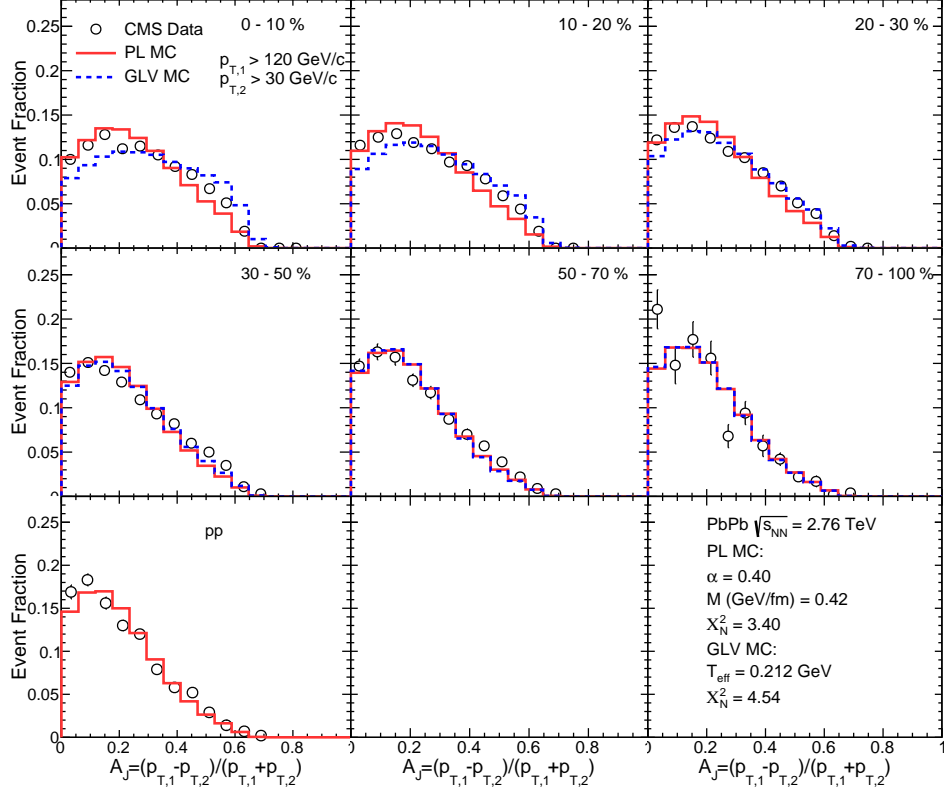


**Fig. 4** (Color online) Dijet asymmetry distribution in different centrality windows in PbPb collisions at  $\sqrt{s_{NN}} = 2.76$  TeV measured by the CMS experiment [11] compared with our calculations using power law and GLV energy loss. The parameters are  $\alpha = 0.40$  and  $M = 0.42$  GeV/fm for PL and  $T_{\text{eff}} = 212$  MeV for GLV.

TeV, respectively. Our estimated values are in agreement with the  $T_{\text{eff}}$  values extracted using the hydrodynamic modelling in ref. [47].

Figure 2 (right) shows transverse size of the system as a function of  $N_{\text{Part}}$  of the collisions. The dashed blue line shows the transverse size,  $R(\tau_0)$ , at the initial time  $\tau_0$  while long dashed red line shows the effective transverse size,  $R^{\text{eff}} = R(\tau_0) + a_t \tau_F^3/6$ , obtained by integrating the  $R(\tau)$  over the time evolution of the system. Table 1 shows the average number of participants, the mean transverse radius of the medium and the mean values of effective path-lengths for the two back-to-back partons in several classes of collision centralities for PbPb collisions at  $\sqrt{s_{NN}} = 2.76$  TeV and 5.02 TeV along with the values of  $R^{\text{eff}}$ . In the peripheral collisions, the transverse plane looks like an ellipse. Since the transverse expansion is faster in the short axis direction, the transverse plane would finally lead to a near circular shape.

Figure 3 shows a snapshot of the transverse cross section of expanding QGP medium of size  $R(\tau)$  at an instant  $\tau$  between initial time  $\tau_0$  and kinetical freeze out time. As seen in Fig. 3 two back-to-back jets produced at radial distance  $r$  could



**Table 1** The average number of participants ( $\langle N_{\text{Part}} \rangle$ ), the mean transverse radius of the medium ( $R^{\text{eff}}$ ) and the mean values of effective path-lengths for the two back-to-back partons ( $\langle L_1 \rangle, \langle L_2 \rangle$ ) in several classes of collision centralities for PbPb collisions at  $\sqrt{s_{NN}} = 2.76$  TeV (I) and at 5.02 TeV (II).

Cent(%)	$\langle N_{\text{Part}} \rangle$		$R^{\text{eff}}$ (fm)		$\langle L_1 \rangle$ (fm)		$\langle L_2 \rangle$ (fm)	
	(I)	(II)	(I)	(II)	(I)	(II)	(I)	(II)
0-10	355	359	8.82	9.20	7.55	7.88	7.70	8.03
10-20	261	264	7.55	7.86	6.45	6.74	6.57	6.86
20-30	187	189	6.40	6.69	5.48	5.70	5.59	5.81
30-40	130	131	5.36	5.58	4.59	4.78	4.67	4.88
40-50	86	87	4.42	4.59	3.78	3.93	3.86	4.01
50-60	54	54	3.52	3.67	3.01	3.12	3.07	3.18
60-70	31	31	2.69	2.79	2.30	2.39	2.34	1.43
70-100	9	9	1.43	1.45	1.23	1.40	1.25	1.43
0-100	113	114	5.01	5.23	4.29	4.45	4.37	4.54

traverse different path-lengths ( $L_1$  and  $L_2$ ) in the medium. The value of freeze out temperature is used as 0.140 GeV in our calculations.

The position  $r$  is generated using a  $2\pi r$  distribution. The directions of the jets given by  $\phi$  in dijet or  $\gamma$ -jet pairs are generated randomly between 0 to  $2\pi$  within the transverse cross section of the medium. The path-lengths  $L_1$  and  $L_2$  can be expressed as

$$\begin{aligned}
 L_1 &= \sqrt{(R^{\text{eff}})^2 - r^2 \sin^2(\phi)} - r \cos(\phi) \\
 L_2 &= \sqrt{(R^{\text{eff}})^2 - r^2 \sin^2(\pi + \phi)} - r \cos(\pi + \phi).
 \end{aligned}
 \tag{10}$$

The path-lengths are kept smaller than the life time of the medium. The energy loss  $\Delta E$  of jets 1 and 2 can be calculated as

$$\Delta E_1 = \frac{dE}{dx} \times L_1, \quad \Delta E_2 = \frac{dE}{dx} \times L_2.
 \tag{11}$$

Note that  $dE/dx$  is also path-lengths ( $L_1, L_2$ ) dependent in case of GLV. If  $p_T$  is the generated transverse momentum of the jet then the final transverse momentum of the jet in dijet or  $\gamma$ -jet pair will be

$$p_{T1} = p_T - \Delta E_1, \quad p_{T2} = p_T - \Delta E_2.$$

The transverse momentum imbalance can be quantified using various asymmetry parameters defined as

$$\begin{aligned}
 A_J &= \frac{p_{T1} - p_{T2}}{p_{T1} + p_{T2}}, \\
 X_J &= \frac{p_{T2}}{p_{T1}}.
 \end{aligned}
 \tag{12}$$

Both these measures are used by experimental groups and these are related to each other as  $A_J = (1 - X_J)/(1 + X_J)$ .

The asymmetry parameter of the  $\gamma$ -jet pairs can be calculated as follows

$$X_{J\gamma} = \frac{p_T^{\text{Jet}}}{p_T^\gamma}. \quad (13)$$

For the  $\gamma$ -jet pairs, no energy loss is assigned for the photon as it does not participate in the strong interaction.

We generate the  $p_T$  of jets using the measured  $p_T$  distribution and the imbalance in  $p_T$  is also obtained using the measured pp data. Thus, the generated  $p_T$  takes into account both the vacuum effect and any experimental effect in pp. For CMS data (Fig. 4, Fig. 5 and Fig. 6) we use the  $p_T$  dependent resolution factor used by the CMS collaboration [17]. The  $p_T$  broadening is taken into account using a Gaussian distribution with width given by experimental resolution multiplied by a constant scale factor ( $\approx 1.7$ ) such that asymmetry distribution in pp collisions are reproduced. The additional broadening in PbPb collisions can then be attributed to energy loss in the medium but it may not be free from experimental effect depending on the experimental setup. The measurements from ATLAS are claimed to account for underlying background and experimental effects [12, 13]. For the ATLAS data (Fig. 7, Fig. 8, Fig. 12 and Fig. 13) the  $p_T$  of one jet is generated using measured  $p_T$  distribution and the  $p_T$  of the other jet is obtained using pp asymmetry distributions.

We also calculate the nuclear modification factor  $R_{AA}$  for jets. ATLAS and CMS experiments measured the  $R_{AA}$  for the jets at  $\sqrt{s_{NN}} = 2.76$  TeV and 5.02 TeV respectively. The dijet events are generated with  $p_T$  distributed as per Eq. 1 and the  $p_T$  of the jets are filled in a histogram  $N_{pp}(p_T)$ . The modified transverse momenta of the two jets after losing energy in the medium are filled in histogram  $N_{PbPb}(p_T)$ . The ratio of the two histograms gives the nuclear modification factor

$$R_{AA} = \frac{N_{PbPb}(p_T)}{N_{pp}(p_T)}. \quad (14)$$

For all the analysis, the experimental cuts are implemented which are  $p_{T1} \geq 120$  GeV/ $c$  and  $p_{T2} \geq 30$  GeV/ $c$  for CMS experiment and  $p_{T1} \geq 100$  GeV/ $c$  and  $p_{T2} \geq 25$  GeV/ $c$  for ATLAS experiment.  $p_T^{\text{Jet}} \geq 30$  GeV/ $c$  and  $p_T^\gamma \geq 60$  GeV/ $c$  for CMS  $\gamma$ -Jet measurement. In addition,  $\Delta\phi \geq 2\pi/3$  for CMS experiment and  $\Delta\phi \geq 7\pi/8$  for ATLAS experiment, where  $\phi$  is the azimuthal angle. The calculations for  $R_{AA}$  does not have the  $\Delta\phi$  cut in accordance to the experimental measurements.

**Table 2** The values of parameters  $\alpha$  and  $M$  extracted from CMS and ATLAS measurements at  $\sqrt{s_{NN}} = 2.76$  TeV and  $\sqrt{s_{NN}} = 5.02$  TeV for Power Law MC method. The value of  $T_{\text{eff}}$  used for GLV MC is also shown.

	$\sqrt{s_{NN}} = 2.76$ TeV		$\sqrt{s_{NN}} = 5.02$ TeV
	CMS ( $A_J, X_J^\gamma$ )	ATLAS ( $X_J, R_{AA}$ )	ATLAS ( $X_J, R_{AA}$ )
$\alpha$	0.40	0.40	0.40
$M$ (GeV/fm)	0.42	0.30	0.32
$T_{\text{eff}}$ (GeV)	0.212	0.212	0.220

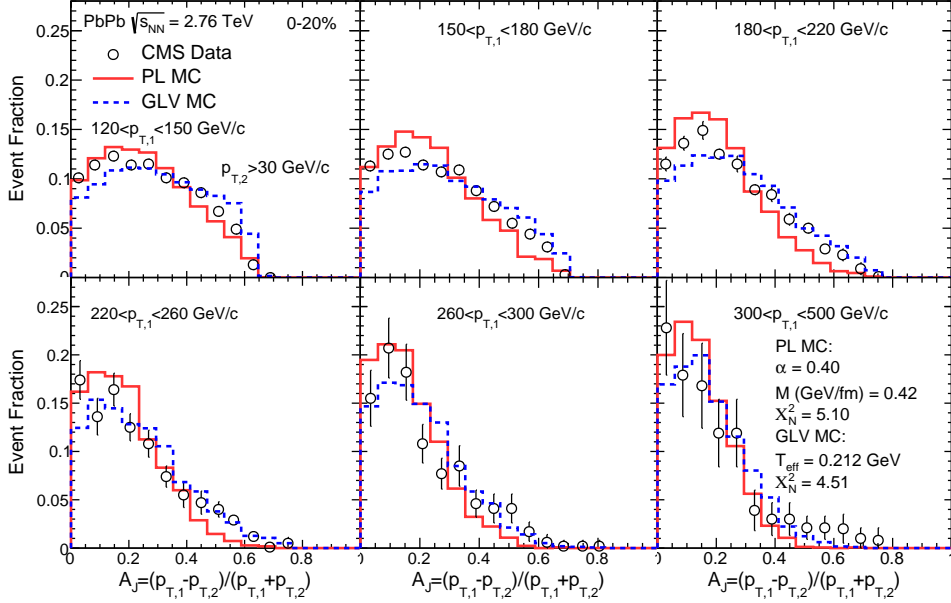


**Fig. 5** (Color online) Dijet asymmetry in different  $p_T$  windows of leading jet in PbPb collisions at  $\sqrt{s_{NN}} = 2.76$  TeV measured by the CMS experiment [16] in 0-20% centrality bin compared with our calculations using power law and GLV energy loss. The parameters are  $\alpha = 0.40$  and  $M = 0.42$  GeV/fm for PL and  $T_{\text{eff}} = 212$  MeV for GLV.

### 3 Results and discussions

We have used two models, Power Law (PL) and GLV to describe the experimental data. While energy loss in case of PL depends on  $L$ , it depends on  $L^2$  for GLV case. In former case the energy loss depends on jet energy by power law and in later case it is logarithmic in jet energy. CMS data of dijet and  $\gamma$ -jet asymmetry in PbPb collisions at  $\sqrt{s_{NN}} = 2.76$  TeV has been used in the analysis. Also ATLAS data of dijet asymmetry and  $R_{AA}$  in PbPb collisions at two energies  $\sqrt{s_{NN}} = 2.76$  TeV and 5.02 TeV have been used. We had aimed to keep two sets of parameters for two collision energies but we did vary them for different experiments and discuss the underlying reason behind it.

Figure 4 shows dijet asymmetry distribution in different centrality windows in PbPb collisions at  $\sqrt{s_{NN}} = 2.76$  TeV measured by the CMS experiment [11] compared with our calculations using power law and GLV energy loss. The parameters obtained for CMS are  $\alpha = 0.40$  and  $M = 0.42$  GeV/fm for PL. The GLV formalism also gives reasonable description of the data using the extracted value of the effective temperature  $T_{\text{eff}} = 212$  MeV. The distributions of  $A_J$  become narrower as we move from central to peripheral collisions, the feature is well produced by both PL and GLV by given parameters with both GLV having slightly higher  $\chi^2/ndf$  values. Figure 5 shows dijet asymmetry in different  $p_T$  windows of leading jet in PbPb collisions at  $\sqrt{s_{NN}} = 2.76$  TeV measured by the CMS experiment [16] in 0-20% centrality bin compared with our calculations using power law and GLV energy loss. The distribution

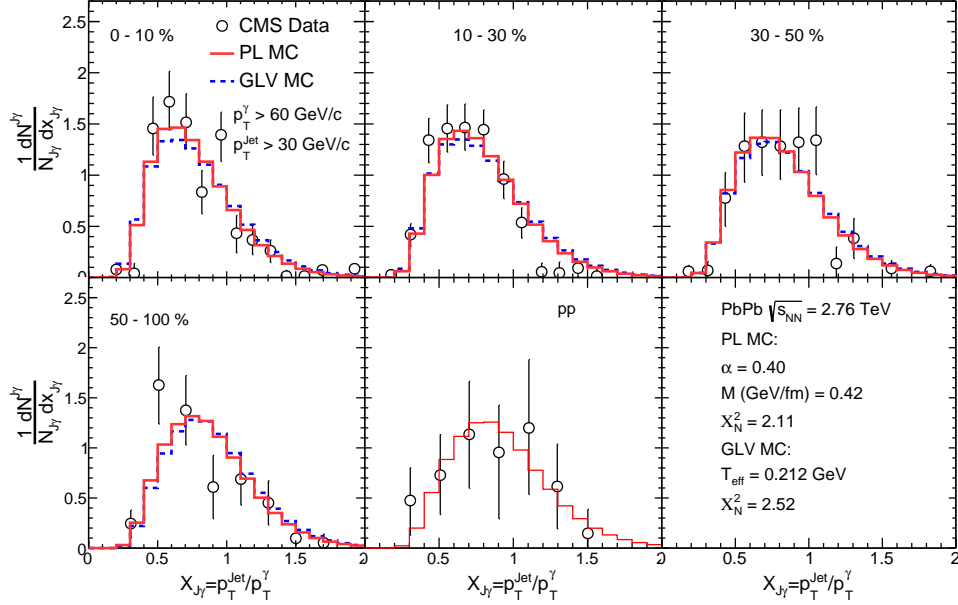


**Fig. 6** (Color online) The  $\gamma$ -jet asymmetry for different centrality regions in PbPb collisions at  $\sqrt{s_{NN}} = 2.76$  TeV as measured by CMS experiment [16] along with the calculations using power law and GLV energy loss. The parameters are  $\alpha = 0.40$  and  $M = 0.42$  GeV/fm for PL and  $T_{\text{eff}} = 212$  MeV for GLV.

becomes narrower as the  $p_T$  of the jets increases, a trend correctly produced by both PL and GLV with above parameters with both models having similar  $\chi^2/ndf$  values. Figure 6 shows the  $\gamma$ -jet asymmetry for different centrality regions in PbPb collisions at  $\sqrt{s_{NN}} = 2.76$  TeV as measured by CMS experiment [16] along with the calculations using power law and GLV energy loss. The same parameters used to describe dijet calculations are able to explain the the  $\gamma$ -jet asymmetry for both PL and GLV within experimental errors. Since the broadening of the asymmetry distribution in case of all CMS data may also include the effect of underlying events, the values of the parameters can be considered as upper limit.

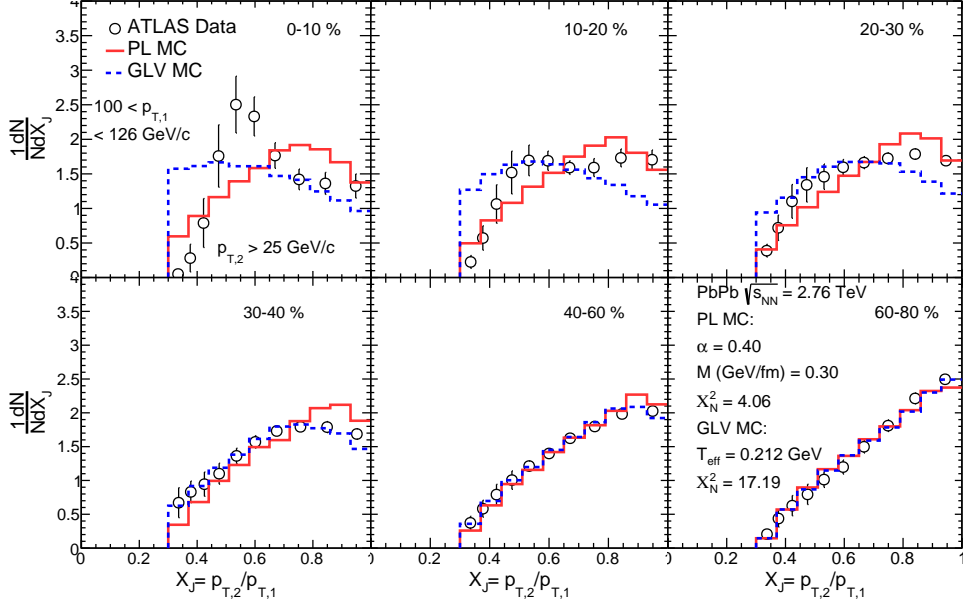
The measurements from ATLAS account for underlying background and experimental effects [12, 13] and thus the shapes of the asymmetry distributions is supposed to arise purely from the energy loss effects. Figure 7 shows the unfolded Di-jet asymmetry ( $X_J$ ) for different  $p_T$  bins in PbPb collisions at  $\sqrt{s_{NN}} = 2.76$  TeV measured by ATLAS experiment [12] along with the calculations using power law and GLV energy loss. The parameters obtained for ATLAS data at  $\sqrt{s_{NN}} = 2.76$  TeV are  $\alpha = 0.40$  and  $M = 0.30$  GeV/fm for PL and  $T_{\text{eff}} = 212$  MeV for GLV. Except the distribution in the lowest  $p_T$  window, the data is well described by PL. The lower values of  $\chi^2/ndf$  for the case of PL show that it describes the data much better as compared to GLV. It can be noted that, the ATLAS data requires smaller values of  $M$  as ATLAS reportedly accounted for experimental effects affecting the broadening of  $X_J$  distributions. Figure 8 shows the unfolded Di-jet asymmetry ( $X_J$ ) for different centrality windows in



**Fig. 7** (Color online) The unfolded Di-jet asymmetry ( $X_J$ ) for different  $p_T$  bins in PbPb collisions at  $\sqrt{s_{NN}} = 2.76$  TeV and in pp collisions at  $\sqrt{s} = 2.76$  TeV measured by ATLAS experiment [12] along with the calculations using power law and GLV energy loss. The parameters used are  $\alpha = 0.40$  and  $M = 0.30$  GeV/fm for PL and  $T_{\text{eff}} = 212$  MeV for GLV.

PbPb collisions at  $\sqrt{s_{NN}} = 2.76$  TeV measured by ATLAS experiment [12] along with the calculations using power law and GLV energy loss. Here also, the lower values of  $\chi^2/ndf$  for the case of PL show that it describes the data much better as compared to GLV. Figure 9 and Fig. 10 shows the jet  $R_{AA}$  as a function of jet  $p_T$  in several collision centrality bins in PbPb collisions at  $\sqrt{s_{NN}} = 2.76$  TeV measured by the ATLAS and CMS experiments [18, 20] respectively. The measurements are compared with the calculations using power law and GLV energy loss. The  $R_{AA}$  value slowly inches towards one as one moves to higher  $p_T$  but, remains below one. The  $R_{AA}$  approaches one as one moves from central to peripheral collisions. The overall dependence of  $R_{AA}$  on  $p_T$  is correctly reproduced by both the models although PL is slightly better in reproducing the trend. The dependence of  $R_{AA}$  on centrality is better described by PL model.

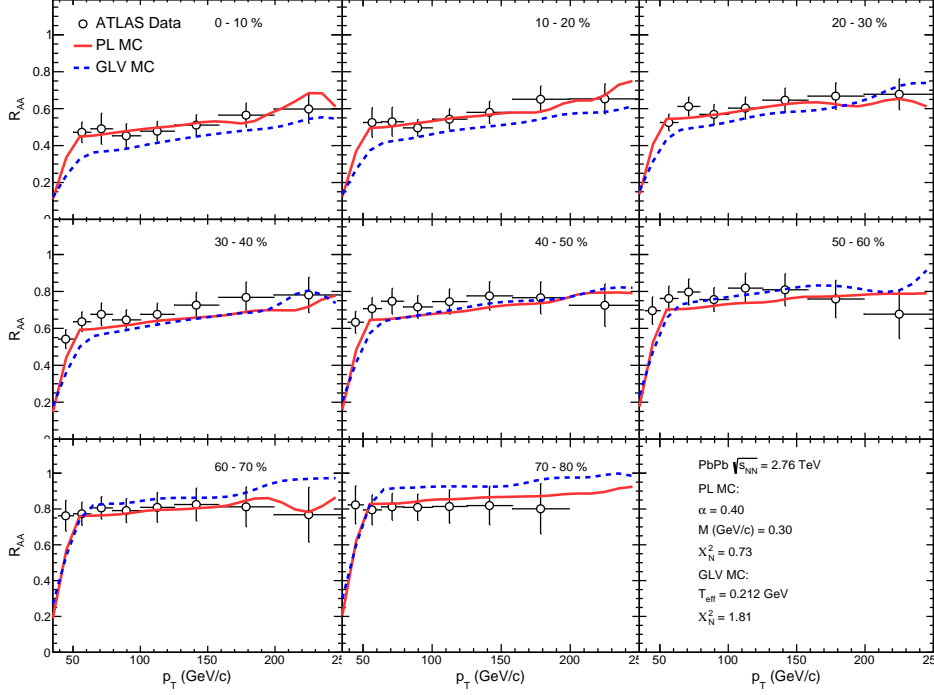
Figure 11 shows the b jet  $R_{AA}$  as a function of jet  $p_T$  in several collision centrality bins in PbPb collisions at  $\sqrt{s_{NN}} = 2.76$  TeV measured by the CMS experiments [48]. The measurements are compared with the calculations using power law and GLV energy loss. The heavy quark initiated jets are expected to lose less energy than the light quark initiated jets due to the dead cone effect [49] however as seen from the Fig. 11 the sensitivity in the data is low due to the large statistical uncertainties on the measurement [48] and the data can be described well with the same parameters those are used for inclusive jets in Fig. 9 and Fig. 10. The value of quark fraction ( $f_q$ ) is taken as unity for the GLV calculations in case of b quark  $R_{AA}$ .



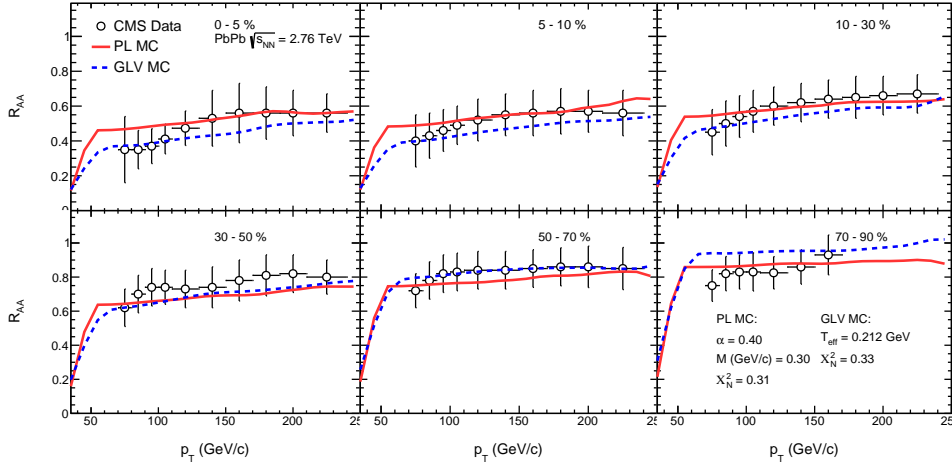
**Fig. 8** (Color online) The unfolded Di-jet asymmetry ( $X_J$ ) for different centrality windows in PbPb collisions at  $\sqrt{s_{NN}} = 2.76$  TeV and in pp collisions at  $\sqrt{s} = 2.76$  TeV measured by ATLAS experiment [12] along with the calculations using power law and GLV energy loss. The parameters used are  $\alpha = 0.40$  and  $M = 0.30$  GeV/fm for PL and  $T_{\text{eff}} = 212$  MeV for GLV.

Figure 12 shows the unfolded Di-jet asymmetry ( $X_J$ ) in different  $p_T$  bins in PbPb collisions at  $\sqrt{s_{NN}} = 5.02$  TeV in the most central 0-10% collisions measured by ATLAS experiment [13] along with the calculations using power law and GLV energy loss. The values of the parameters obtained for ATLAS experiment at  $\sqrt{s_{NN}} = 5.02$  TeV are  $\alpha = 0.40$  and  $M = 0.32$  GeV/fm for PL and  $T_{\text{eff}} = 220$  MeV for GLV which are more as compared to the case for  $\sqrt{s_{NN}} = 2.76$  TeV showing more energy loss of jets at higher collisions energy. Figure 13 shows the unfolded Di-jet asymmetry ( $X_J$ ) in different  $p_T$  bins in PbPb collisions at  $\sqrt{s_{NN}} = 5.02$  TeV in the peripheral 40-60% collisions measured by ATLAS experiment [13] along with the calculations using power law and GLV energy loss. The Fig. 12 and Fig. 13 show that PL describe the data much better than the GLV formalism. Figure 14 shows the jet  $R_{AA}$  as a function of jet  $p_T$  in several collision centrality bins in PbPb collisions at  $\sqrt{s_{NN}} = 5.02$  TeV measured by the ATLAS experiment [19]. The measurements are compared with calculations using power law and GLV energy loss. The dependence of  $R_{AA}$  on  $p_T$  and centrality is described by both the models within the experimental errors.

Table 2 summarises the values of parameters used to describe  $A_J$  and  $X_J^\gamma$  by CMS experiment at  $\sqrt{s_{NN}} = 2.76$  TeV and  $X_J$  and  $R_{AA}$  by ATLAS experiments at  $\sqrt{s_{NN}} = 2.76$  TeV and  $\sqrt{s_{NN}} = 5.02$  TeV. In principle, we should need only two sets of values for parameters  $\alpha$  and  $M$  for two energies. The CMS data of  $A_J$  and  $X_J^\gamma$  requires larger values of  $M$  as compared to ATLAS data. The experimental effects might contribute to the broadening of  $X_J$  distributions mimicking larger energy loss.



**Fig. 9** (Color online) Jet  $R_{AA}$  as a function of jet  $p_T$  in several collision centrality bins in PbPb collisions at  $\sqrt{s_{NN}} = 2.76$  TeV measured by the ATLAS experiment [18]. The measurements are compared calculations using power law and GLV energy loss. The parameters used are  $\alpha = 0.40$  and  $M = 0.30$  GeV/fm for PL and  $T_{\text{eff}} = 212$  MeV for GLV.



**Fig. 10** (Color online) Jet  $R_{AA}$  as a function of jet  $p_T$  in several collision centrality bins in PbPb collisions at  $\sqrt{s_{NN}} = 2.76$  TeV measured by the CMS experiment [20]. The measurements are compared calculations using power law and GLV energy loss. The parameters used are  $\alpha = 0.40$  and  $M = 0.30$  GeV/fm for PL and  $T_{\text{eff}} = 212$  MeV for GLV.

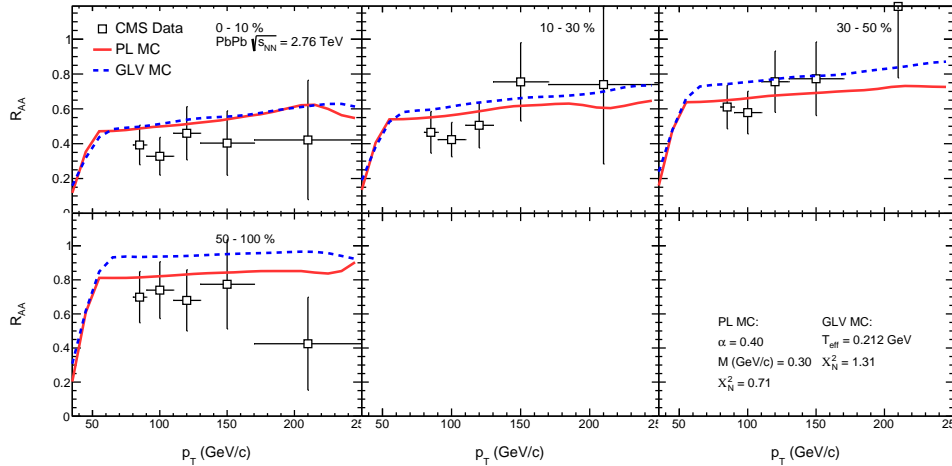


**Fig. 11** (Color online) b-Jet  $R_{AA}$  as a function of jet  $p_T$  in several collision centrality bins in PbPb collisions at  $\sqrt{s_{NN}} = 2.76$  TeV measured by the CMS experiment [48]. The measurements are compared calculations using power law and GLV energy loss. The parameters used are  $\alpha = 0.40$  and  $M = 0.30$  GeV/fm for PL and  $T_{\text{eff}} = 212$  MeV for GLV.

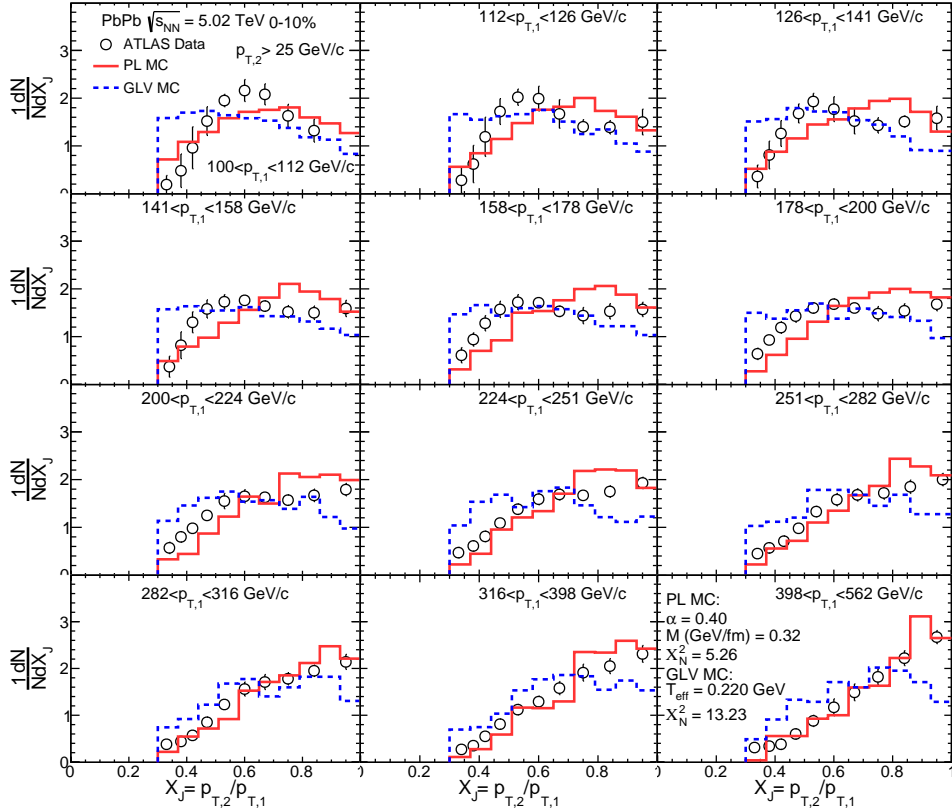
The ATLAS experiment reportedly removes the effects of experimental resolution and underlying event to appear in their measured  $X_J$  spectra. The extracted values of  $\alpha$  are slightly smaller than the  $\sqrt{E}$  dependence expected from the BDPS formalism [2]. The parametric analysis from Ref. [33] gives the value of this index as 0.52. Our analysis show that the energy loss of jets increases less rapidly with the jet energy than expected from  $\sqrt{E}$  dependence. The value of  $T_{\text{eff}}$  is more for higher collision energy which is expected to create a system at higher temperature. The value of  $M$  in PL is also dependent on the temperature of the system and is larger for higher collision energy.

Figure 15 shows energy loss per unit length,  $dE/dx$ , as a function of jet  $p_T$  in central 0-10% and peripheral 50-60% collisions for both PL and GLV models. The value of  $dE/dx$  is more for GLV in the 0-10% centrality bin while for 50-60% bin the value for GLV method is smaller because of small  $L_{\text{eff}}$ . This difference in energy loss dependence of centrality in the two models is visible in figures 9 and 14. The value of  $dE/dx$  increases slowly as a function of jet  $p_T$  for both PL and GLV models. This gives a slightly increasing trend in  $R_{AA}$  as a function of  $p_T$  as shown in figures 9 and 14. Overall,  $p_T$  and centrality dependence of  $R_{AA}$  and asymmetry is described better by PL model as compared to GLV.

## 4 Summary

In this work, we quantify the jet energy loss in the medium using a variety of jet energy loss observables. The calculations are performed using specific energy loss,  $dE/dx$ , having jet energy dependence to be a power law form (PL) or logarithmic form (GLV). A Monte Carlo model is employed to obtain transverse momentum  $p_T$  and path-lengths of the initial jets which suffer energy loss in the medium using the





**Fig. 12** (Color online) The unfolded Di-jet asymmetry ( $X_J$ ) in different  $p_T$  bins in PbPb collisions at  $\sqrt{s_{NN}} = 5.02$  TeV in the most central 0-10% collisions measured by ATLAS experiment [13] along with the calculations using power law and GLV energy loss. The parameters used are  $\alpha = 0.40$  and  $M = 0.32$  GeV/fm for PL and  $T_{\text{eff}} = 220$  MeV for GLV.

above functional forms. The dijet asymmetry distributions and nuclear modification factors  $R_{AA}$  are calculated and compared with the CMS and ATLAS measurements in Pb+Pb collisions at energies  $\sqrt{s_{NN}} = 2.76$  TeV and 5.02 TeV. The dijet asymmetry distributions broaden as the  $p_T$  of the leading jet increases and/or the collisions are more central, a trend which is reproduced by Monte Carlo model. The shapes of asymmetry distributions in all kinematics regions are better described by power law as compared to GLV form. The data from CMS requires larger energy loss as compared to ATLAS data to explain the broadening of the asymmetry ( $A_J/X_J$ ) distributions signifying the importance of removing experimental effects on the broadening. The energy loss increases slightly as one moves from the collision energy  $\sqrt{s_{NN}} = 2.76$  TeV to 5.02 TeV as the medium created at higher energy is supposed to have larger temperature. While, the dependence of  $R_{AA}$  on  $p_T$  is correctly reproduced by both the power law and GLV forms, the dependence of  $R_{AA}$  on centrality is slightly better described by PL model. This indicates the dependence of energy loss on jet energy

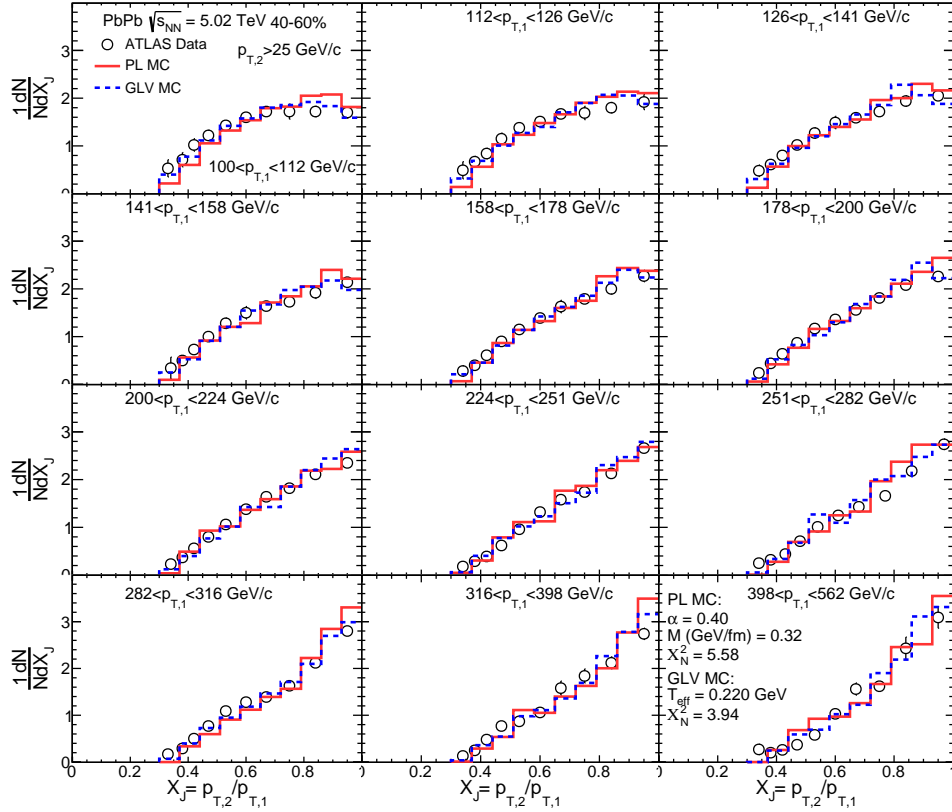


**Fig. 13** (Color online) The unfolded Di-jet asymmetry ( $X_J$ ) in different  $p_T$  bins in PbPb collisions at  $\sqrt{s_{NN}} = 5.02$  TeV in the peripheral 40-60% collisions measured by ATLAS experiment [13] along with the calculations using power law and GLV energy loss. The parameters used are  $\alpha = 0.40$  and  $M = 0.32$  GeV/fm for PL and  $T_{\text{eff}} = 220$  MeV for GLV.

and path-length is better described by PL model. The method can be used to predict the jet  $R_{AA}$  and dijet asymmetry values in heavy ion collisions for future experiments.

## References

- [1] Busza, W., Rajagopal, K., Schee, W.: Heavy ion collisions: The big picture and the big questions. Annual Review of Nuclear and Particle Science **68**(1), 339–376 (2018) <https://doi.org/10.1146/annurev-nucl-101917-020852>
- [2] Baier, R., Dokshitzer, Y.L., Peigne, S., Schiff, D.: Induced gluon radiation in a QCD medium. Phys. Lett. B **345**, 277–286 (1995) [https://doi.org/10.1016/0370-2693\(94\)01617-L](https://doi.org/10.1016/0370-2693(94)01617-L) arXiv:hep-ph/9411409
- [3] Gyulassy, M., Plumer, M.: Jet Quenching in Dense Matter. Phys. Lett. B **243**, 432–438 (1990) [https://doi.org/10.1016/0370-2693\(90\)91409-5](https://doi.org/10.1016/0370-2693(90)91409-5)

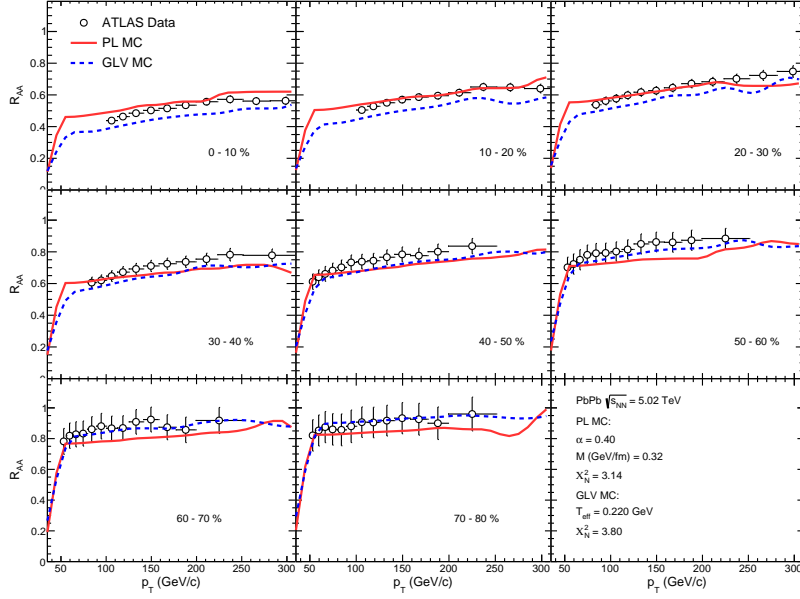


**Fig. 14** (Color online) Jet  $R_{AA}$  as a function of jet  $p_T$  in several collision centrality bins in PbPb collisions at  $\sqrt{s_{NN}} = 5.02$  TeV measured by the ATLAS experiment [19]. The measurements are compared with calculations using power law and GLV energy loss. The parameters used are  $\alpha = 0.40$  and  $M = 0.32$  GeV/fm for PL and  $T_{\text{eff}} = 220$  MeV for GLV.

- [4] Bjorken, J.D.: Energy Loss of Energetic Partons in Quark - Gluon Plasma: Possible Extinction of High  $p_T$  Jets in Hadron - Hadron Collisions (1982)
- [5] Adams, J., *et al.*: Transverse momentum and collision energy dependence of high  $p_T$  hadron suppression in Au+Au collisions at ultrarelativistic energies. Phys. Rev. Lett. **91**, 172302 (2003) <https://doi.org/10.1103/PhysRevLett.91.172302> [arXiv:nucl-ex/0305015](https://arxiv.org/abs/nucl-ex/0305015)
- [6] Aamodt, K., *et al.*: Suppression of Charged Particle Production at Large Transverse Momentum in Central Pb-Pb Collisions at  $\sqrt{s_{NN}} = 2.76$  TeV. Phys. Lett. B **696**, 30–39 (2011) <https://doi.org/10.1016/j.physletb.2010.12.020> [arXiv:1012.1004](https://arxiv.org/abs/1012.1004) [nucl-ex]
- [7] Chatrchyan, S., *et al.*: Study of high- $p_T$  charged particle suppression in PbPb compared to  $pp$  collisions at  $\sqrt{s_{NN}} = 2.76$  TeV. Eur. Phys. J. C **72**, 1945 (2012) <https://doi.org/10.1140/epjc/s10052-012-1945-x> [arXiv:1202.2554](https://arxiv.org/abs/1202.2554) [nucl-ex]
- [8] Khachatryan, V., *et al.*: Charged-particle nuclear modification factors in PbPb and pPb collisions at  $\sqrt{s_{NN}} = 5.02$  TeV. JHEP **04**, 039 (2017) [https://doi.org/10.1007/JHEP04\(2017\)039](https://doi.org/10.1007/JHEP04(2017)039) [arXiv:1611.01664](https://arxiv.org/abs/1611.01664) [nucl-ex]

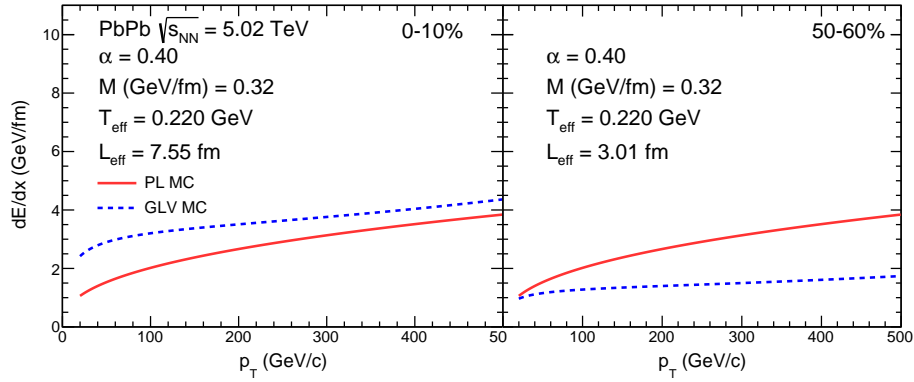


**Fig. 15** (Color online) The energy loss per unit length,  $dE/dx$ , as a function of jet  $p_T$  in central (0-10%) and peripheral (50-60%) collisions for both PL and GLV models.

- [9] Aad, G., *et al.*: Observation of a Centrality-Dependent Dijet Asymmetry in Lead-Lead Collisions at  $\sqrt{s_{NN}} = 2.77$  TeV with the ATLAS Detector at the LHC. *Phys. Rev. Lett.* **105**, 252303 (2010) <https://doi.org/10.1103/PhysRevLett.105.252303> [arXiv:1011.6182](https://arxiv.org/abs/1011.6182) [hep-ex]
- [10] Chatrchyan, S., *et al.*: Observation and studies of jet quenching in PbPb collisions at nucleon-nucleon center-of-mass energy 2.76 TeV. *Phys. Rev. C* **84**, 024906 (2011) <https://doi.org/10.1103/PhysRevC.84.024906> [arXiv:1102.1957](https://arxiv.org/abs/1102.1957) [nucl-ex]
- [11] Chatrchyan, S., *et al.*: Jet momentum dependence of jet quenching in PbPb collisions at  $\sqrt{s_{NN}} = 2.76$  TeV. *Phys. Lett. B* **712**, 176–197 (2012) <https://doi.org/10.1016/j.physletb.2012.04.058> [arXiv:1202.5022](https://arxiv.org/abs/1202.5022) [nucl-ex]
- [12] Aaboud, M., *et al.*: Measurement of jet  $p_T$  correlations in Pb+Pb and  $pp$  collisions at  $\sqrt{s_{NN}} = 2.76$  TeV with the ATLAS detector. *Phys. Lett. B* **774**, 379–402 (2017) <https://doi.org/10.1016/j.physletb.2017.09.078> [arXiv:1706.09363](https://arxiv.org/abs/1706.09363) [hep-ex]
- [13] Aad, G., *et al.*: Measurements of the suppression and correlations of dijets in Pb+Pb collisions at  $s_{NN}=5.02$  TeV. *Phys. Rev. C* **107**(5), 054908 (2023) <https://doi.org/10.1103/PhysRevC.107.054908> [arXiv:2205.00682](https://arxiv.org/abs/2205.00682) [nucl-ex]
- [14] Aad, G., *et al.*: Measurement of substructure-dependent jet suppression in Pb+Pb collisions at 5.02 TeV with the ATLAS detector. *Phys. Rev. C* **107**(5), 054909 (2023) <https://doi.org/10.1103/PhysRevC.107.054909> [arXiv:2211.11470](https://arxiv.org/abs/2211.11470) [nucl-ex]
- [15] Adamczyk, L., *et al.*: Dijet imbalance measurements in  $Au + Au$  and  $pp$  collisions at  $\sqrt{s_{NN}} = 200$  GeV at STAR. *Phys. Rev. Lett.* **119**(6), 062301 (2017) <https://doi.org/10.1103/PhysRevLett.119.062301> [arXiv:1609.03878](https://arxiv.org/abs/1609.03878) [nucl-ex]

- [16] Chatrchyan, S., *et al.*: Studies of jet quenching using isolated-photon+jet correlations in PbPb and  $pp$  collisions at  $\sqrt{s_{NN}} = 2.76$  TeV. Phys. Lett. B **718**, 773–794 (2013) <https://doi.org/10.1016/j.physletb.2012.11.003> arXiv:1205.0206 [nucl-ex]
- [17] Sirunyan, A.M., *et al.*: Study of Jet Quenching with  $Z$ +jet Correlations in Pb-Pb and  $pp$  Collisions at  $\sqrt{s_{NN}} = 5.02$ TeV. Phys. Rev. Lett. **119**(8), 082301 (2017) <https://doi.org/10.1103/PhysRevLett.119.082301> arXiv:1702.01060 [nucl-ex]
- [18] Aad, G., *et al.*: Measurements of the Nuclear Modification Factor for Jets in Pb+Pb Collisions at  $\sqrt{s_{NN}} = 2.76$  TeV with the ATLAS Detector. Phys. Rev. Lett. **114**(7), 072302 (2015) <https://doi.org/10.1103/PhysRevLett.114.072302> arXiv:1411.2357 [hep-ex]
- [19] Aaboud, M., *et al.*: Measurement of the nuclear modification factor for inclusive jets in Pb+Pb collisions at  $\sqrt{s_{NN}} = 5.02$  TeV with the ATLAS detector. Phys. Lett. B **790**, 108–128 (2019) <https://doi.org/10.1016/j.physletb.2018.10.076> arXiv:1805.05635 [nucl-ex]
- [20] Khachatryan, V., *et al.*: Measurement of inclusive jet cross sections in  $pp$  and PbPb collisions at  $\sqrt{s_{NN}} = 2.76$  TeV. Phys. Rev. C **96**(1), 015202 (2017) <https://doi.org/10.1103/PhysRevC.96.015202> arXiv:1609.05383 [nucl-ex]
- [21] Gyulassy, M., Levai, P., Vitev, I.: NonAbelian energy loss at finite opacity. Phys. Rev. Lett. **85**, 5535–5538 (2000) <https://doi.org/10.1103/PhysRevLett.85.5535> arXiv:nucl-th/0005032
- [22] Gyulassy, M., Levai, P., Vitev, I.: Reaction operator approach to nonAbelian energy loss. Nucl. Phys. B **594**, 371–419 (2001) [https://doi.org/10.1016/S0550-3213\(00\)00652-0](https://doi.org/10.1016/S0550-3213(00)00652-0) arXiv:nucl-th/0006010
- [23] Baier, R., Dokshitzer, Y.L., Mueller, A.H., Peigne, S., Schiff, D.: Radiative energy loss of high-energy quarks and gluons in a finite volume quark - gluon plasma. Nucl. Phys. B **483**, 291–320 (1997) [https://doi.org/10.1016/S0550-3213\(96\)00553-6](https://doi.org/10.1016/S0550-3213(96)00553-6) arXiv:hep-ph/9607355
- [24] Baier, R., Dokshitzer, Y.L., Mueller, A.H., Peigne, S., Schiff, D.: Radiative energy loss and  $p(T)$  broadening of high-energy partons in nuclei. Nucl. Phys. B **484**, 265–282 (1997) [https://doi.org/10.1016/S0550-3213\(96\)00581-0](https://doi.org/10.1016/S0550-3213(96)00581-0) arXiv:hep-ph/9608322
- [25] Muller, B.: Phenomenology of jet quenching in heavy ion collisions. Phys. Rev. C **67**, 061901 (2003) <https://doi.org/10.1103/PhysRevC.67.061901> arXiv:nucl-th/0208038
- [26] Peigné, S., Smilga, A.V.: Energy losses in relativistic plasmas: QCD versus QED. Physics-Uspekhi **52**(7), 659–685 (2009) <https://doi.org/10.3367/ufne.0179.200907a.0697>

- [27] Baier, R., Schiff, D., Zakharov, B.G.: Energy loss in perturbative QCD. Annual Review of Nuclear and Particle Science **50**(1), 37–69 (2000) <https://doi.org/10.1146/annurev.nucl.50.1.37>
- [28] De, S., Srivastava, D.K.: Nuclear modification of charged hadron production at the LHC. J. Phys. G **40**, 075106 (2013) <https://doi.org/10.1088/0954-3899/40/7/075106> [arXiv:1112.2492](https://arxiv.org/abs/1112.2492) [nucl-th]
- [29] De, S., Srivastava, D.K.: System size dependence of nuclear modification and azimuthal anisotropy of jet quenching. J. Phys. G **39**, 015001 (2012) <https://doi.org/10.1088/0954-3899/39/1/015001> [arXiv:1107.5659](https://arxiv.org/abs/1107.5659) [nucl-th]. [Erratum: J.Phys.G 40, 049502 (2013)]
- [30] Caucal, P., Iancu, E., Mueller, A.H., Soyez, G.: Vacuum-like jet fragmentation in a dense QCD medium. Phys. Rev. Lett. **120**, 232001 (2018) <https://doi.org/10.1103/PhysRevLett.120.232001> [arXiv:1801.09703](https://arxiv.org/abs/1801.09703) [hep-ph]
- [31] Caucal, P., Iancu, E., Soyez, G.: Deciphering the  $z_g$  distribution in ultrarelativistic heavy ion collisions. JHEP **10**, 273 (2019) [https://doi.org/10.1007/JHEP10\(2019\)273](https://doi.org/10.1007/JHEP10(2019)273) [arXiv:1907.04866](https://arxiv.org/abs/1907.04866) [hep-ph]
- [32] Mehtar-Tani, Y., Pablos, D., Tywoniuk, K.: Cone-Size Dependence of Jet Suppression in Heavy-Ion Collisions. Phys. Rev. Lett. **127**(25), 252301 (2021) <https://doi.org/10.1103/PhysRevLett.127.252301> [arXiv:2101.01742](https://arxiv.org/abs/2101.01742) [hep-ph]
- [33] Spousta, M.: On similarity of jet quenching and charmonia suppression. Phys. Lett. B **767**, 10–15 (2017) <https://doi.org/10.1016/j.physletb.2017.01.041> [arXiv:1606.00903](https://arxiv.org/abs/1606.00903) [hep-ph]
- [34] Ringer, F., Xiao, B.-W., Yuan, F.: Can we observe jet  $p_T$ -broadening in heavy-ion collisions at the LHC? Phys. Lett. B **808**, 135634 (2020) <https://doi.org/10.1016/j.physletb.2020.135634> [arXiv:1907.12541](https://arxiv.org/abs/1907.12541) [hep-ph]
- [35] Ortiz, A., Vázquez, O.: Energy density and path-length dependence of the fractional momentum loss in heavy-ion collisions at  $\sqrt{s_{NN}}$  from 62.4 to 5020 GeV. Phys. Rev. C **97**(1), 014910 (2018) <https://doi.org/10.1103/PhysRevC.97.014910> [arXiv:1708.07571](https://arxiv.org/abs/1708.07571) [hep-ph]
- [36] Saraswat, K., Shukla, P., Singh, V.: Transverse momentum spectra of hadrons in high energy pp and heavy ion collisions. J. Phys. Comm. **2**(3), 035003 (2018) <https://doi.org/10.1088/2399-6528/aab00f> [arXiv:1706.04860](https://arxiv.org/abs/1706.04860) [hep-ph]
- [37] Shukla, P., Saraswat, K.: Understanding partonic energy loss from measured light charged particles and jets in PbPb collisions at LHC energies. J. Phys. G **47**(12), 125103 (2020) <https://doi.org/10.1088/1361-6471/abb58a> [arXiv:2105.06364](https://arxiv.org/abs/2105.06364) [hep-ph]

- [38] Kumar, A., *et al.*: Inclusive jet and hadron suppression in a multistage approach. Phys. Rev. C **107**(3), 034911 (2023) <https://doi.org/10.1103/PhysRevC.107.034911> arXiv:2204.01163 [hep-ph]
- [39] Hagedorn, R.: Multiplicities,  $p_T$  Distributions and the Expected Hadron  $\rightarrow$  Quark - Gluon Phase Transition. Riv. Nuovo Cim. **6N10**, 1–50 (1983) <https://doi.org/10.1007/BF02740917>
- [40] Sjöstrand, T., Ask, S., Christiansen, J.R., Corke, R., Desai, N., Ilten, P., Mrenna, S., Prestel, S., Rasmussen, C.O., Skands, P.Z.: An introduction to PYTHIA 8.2. Comput. Phys. Commun. **191**, 159–177 (2015) <https://doi.org/10.1016/j.cpc.2015.01.024> arXiv:1410.3012 [hep-ph]
- [41] Spousta, M., Cole, B.: Interpreting single jet measurements in Pb + Pb collisions at the LHC. Eur. Phys. J. C **76**(2), 50 (2016) <https://doi.org/10.1140/epjc/s10052-016-3896-0> arXiv:1504.05169 [hep-ph]
- [42] Kumar, V., Shukla, P., Bhattacharyya, A.: Suppression of quarkonia in pbpb collisions at  $\sqrt{s_{NN}} = 5.02$  tev. J. of Phys G **47**(1), 015104 (2019) <https://doi.org/10.1088/1361-6471/ab51cf>
- [43] Kumar, V., Shukla, P., Vogt, R.: Quarkonia suppression in PbPb collisions at  $\sqrt{s_{NN}} = 2.76$  TeV. Phys. Rev. C **92**(2), 024908 (2015) <https://doi.org/10.1103/PhysRevC.92.024908> arXiv:1410.3299 [hep-ph]
- [44] Huovinen, P., Petreczky, P.: QCD Equation of State and Hadron Resonance Gas. Nucl. Phys. A **837**, 26–53 (2010) <https://doi.org/10.1016/j.nuclphysa.2010.02.015> arXiv:0912.2541 [hep-ph]
- [45] Shuryak, E.V.: Two stage equilibration in high-energy heavy ion collisions. Phys. Rev. Lett. **68**, 3270–3272 (1992) <https://doi.org/10.1103/PhysRevLett.68.3270>
- [46] Adam, J., *et al.*: Centrality Dependence of the Charged-Particle Multiplicity Density at Midrapidity in Pb-Pb Collisions at  $\sqrt{s_{NN}} = 5.02$  TeV. Phys. Rev. Lett. **116**(22), 222302 (2016) <https://doi.org/10.1103/PhysRevLett.116.222302> arXiv:1512.06104 [nucl-ex]
- [47] Gardim, F.G., Giacalone, G., Luzum, M., Ollitrault, J.-Y.: Thermodynamics of hot strong-interaction matter from ultrarelativistic nuclear collisions. Nature Phys. **16**(6), 615–619 (2020) <https://doi.org/10.1038/s41567-020-0846-4> arXiv:1908.09728 [nucl-th]
- [48] Chatrchyan, S., *et al.*: Evidence of b-Jet Quenching in PbPb Collisions at  $\sqrt{s_{NN}} = 2.76$  TeV. Phys. Rev. Lett. **113**(13), 132301 (2014) <https://doi.org/10.1103/PhysRevLett.113.132301> arXiv:1312.4198 [nucl-ex]. [Erratum: Phys.Rev.Lett. 115, 029903 (2015)]

- [49] Dokshitzer, Y.L., Kharzeev, D.E.: Heavy quark colorimetry of QCD matter. Phys. Lett. B **519**, 199–206 (2001) [https://doi.org/10.1016/S0370-2693\(01\)01130-3](https://doi.org/10.1016/S0370-2693(01)01130-3)  
[arXiv:hep-ph/0106202](https://arxiv.org/abs/hep-ph/0106202)